Bachelor Degree Project

UNIVERSITY OF SKÖVDE

INFLAMMASOME

Investigating the effect of NEK7 in the activation of the NLRP3 Inflammasome

Bachelor Degree Project in Bioscience
Level ECTS: 30
Spring term: 2020

Author: Cosmas Adindu Uzowuru
Email: a17cosuz@student.his.se

Supervisor: Mikael Ejdebäck
Email: mikael.ejdeback@his.se

Supervisor: Matthew Herring
Email: matthew.herring@his.se

Examiner: Maria Algerin
Email: maria.algerin@his.se

Abstrct

Inflammation is a biological defence mechanism applied by living organisms against foreign invaders. In the response to DAMPs and PAMPs, organisms use inflammatory multi-protein complexes to fight the attackers. The most studied inflammasome proteins are NLRP3, ASC and Caspase-1. This study is aimed at understanding the role of NEK7 protein in the NLRP3 inflammasome's activation, using CRISPR/Cas9 system. To determine the effect of CRISPR/Cas9 and transfection, mRNA expression was analyzed. The results obtained suggest that neither the transfection nor the NEK7 protein knockout have sufficiently worked. This study could not experimentally establish that NEK7 triggers NLRP3 inflammasome activation because ELISA was not conducted to verify the levels of cytokines emitted, due to there being no statistical differences between the samples. Above all, the research question in this thesis project was not answered because the instability of the ACTB reference gene negatively influenced the results. However, previous related studies conclude that NEK7 plays a crucial role in the activation of the NLRP3 inflammasome.

Keywords: NLRP3 inflammasome, NEK7 protein, THP-1, Prime, activate, differentiate, stimulate, cytokines, Interleukin-1 Beta, Interleukin-18.

Abbreviations

AIM2	Absent-in-melanoma 2
ASC	Apoptosis-associated speck-like protein containing a caspase-recruitment domain
BRCC36	BRCA1-BRCA2-containing complex
CAPS	cryopyrin-associated periodic syndromes
CU	Control-transfected, un-primed
CP	Control-transfected, primed
CPA	Control-transfected, primed and activated
DAMPs	Damage-associated molecular patterns
GSDMD	Gasdermin D
HIN	200-amino-acid domain
LPS	Lipopolysaccharide
LRR	Leucine-rich repeat
MYD88	Myeloid differentiation primary response 88
NEK7	Never in mitosis A-related kinase 7
NF-Kb	Nuclear factor kappa-light-chain-enhancer of activated B cells
NLR	Nod-like receptor
NLRP3	Nod-like receptor pyrin domain containing 3
NOD	Nucleotide-binding oligomerization domain
NU	Non-transfected, un-primed
NP	Non-transfected, primed
NPA	Non-transfected, primed and activated
PAMPs	Pathogen-associated molecular patterns
PRR	Pattern-recognition receptor
PYD	Pyrin domain
TLR	Toll-like receptors
TRIF	TIR-domain-containing adapter-inducing interferon-β
TU	Transfected, un-primed
TP	Transfected primed
TPA	Transfected, primed and activated

Table of Contents

Introduction

Inflammation, inflammasomes and defence mechanism

Inflammation is one of the body's defence systems that participates in the healing mechanism (Medzhitov, 2008; Medical News Today, 2020). The immune system instigates a biological response to combat an invader when detected. The intruders could be thorns, irritants and pathogens, among others. The pathogens are bacteria, viruses and any organism that generates infections. Inflammation could cause chronic diseases, such as metabolic syndromes, which include obesity, type 2 diabetes and heart diseases. Additionally, inflammation could lead to autoimmune diseases, such as type 1 diabetes, by making the body accidentally recognise its own cells and tissues as destructive (Medzhitov, 2008; Medical News Today, 2020).

In the innate immune system the inflammasomes operate by means of the germline-encoded pattern-recognition receptors (PRRs) that activate inflammasomes in reaction to toxic stimuli, such as infecting pathogens, dead cells, and environmental irritants (Kelley, Jeltema, Duan, & He, 2019). Inflammasomes are clusters of immune machinery consisting of multi-protein complexes, comprised of NLR and PYHIN proteins, including NLRP1, NLRP3, NLRC4 and AIM2 (Henao-Mejia, et al., 2012). Another way to describe it, is that inflammasomes, thanks to the PRRs, are antennas detecting exogenous pathogen-associated molecular patterns (PAMPs) or endogenous damage-associated molecular patterns (DAMPs) that control the cleavage of effector pro-inflammatory cytokines such as pro-IL-Iβ and pro-IL-18 (Henao-Mejia et al., 2012).

Inflammatory formation and recognition mechanism

In reaction to the invaders, the inflammatory proteins, such as NLRP3, ASC and caspase-1, oligomerize to activate the inflammatory complex, purposely to eradicate infectious contaminations and repair damaged tissues (Kelley et al., 2019). To activate inflammasomes, multi-intracellular protein complexes, including ASC as an adaptor between the NLR family and PYHIN, activate caspase-1 which forms the activated inflammatory complex (Franchi, Eigenbrod, Muñoz-Planillo, & Nuñez, 2009). The key established PRRs in the formation of inflammasomes, such as nucleotide-binding oligomerization domain (NOD), leucine-rich repeat (LRR)-comprising proteins (NLR) family members, the absent-in-melanoma 2 (AIM2) and the pyrin/PYHIN (Sharma & Kanneganti, 2016; Lamkanfi & Dixit, 2014)

An apoptosis-associated speck-like protein containing a caspase-recruitment domain (ASC), is a two ways adaptor protein that plays an important role in connecting pro-caspase-1 to the inflammasome complex (Fernandes-Alnemri et al., 2007). Caspase-1 is activated when it comes in close contact with the inflammasome using a proximity-induced autocatalytic activation (Kelley et al., 2019). The cytokines, mostly pro-interleukin-1β (pro-IL-1β) and pro-IL-18 are induced to their mature and biologically active forms, when the active caspase-1 cleaves them. The IL-1β then triggers the expression of genes that regulate fever, pain threshold, vasodilation, and hypotension. This reaction starts a response from an endothelial cell which facilitates the penetration of immune cells into infected and damaged tissues. The IL-18, in turn, is responsible for interferon-gamma (IFN-Ɣ) formation and is one of the cytokines that facilitate adaptive immunity (Dinarello, 2009).

An active caspase-1 cleaves gasdermin D (GSDMD), resulting in the N-terminal domain of GSDMD to produce holes in the plasma membrane, hence inducing pyroptosis. The pyroptosis in this scenario, has a biological importance in that it forces intracellular pathogens away from their replicative position, subjecting them to other immune components, and also induces the release

of cytokines and the generation of DAMPs to enhance the immune system's response to contamination or infection (Fink & Cookson, 2006; He, Wan, Chen et al., 2015; Miao et al., 2010)

NLRP3 inflammasome

The NLRP3 inflammasome poses an essential immune defence against bacterial, fungal, and viral infections (Thomas et al., 2009). Numerous inflammatory disorders such as cryopyrin-associated periodic syndromes (CAPS), Alzheimer's disease, diabetes, gout, autoinflammatory diseases, and atherosclerosis is connected to the dysregulation of the NLRP3 inflammasome (Menu & Vince, 2011; Guo, Callaway & Ting, 2015). The NLRP3 inflammasome is a multilateral protein that comprises of an amino-terminal pyrin domain (PYD), a central nucleotide-binding and oligomerization domain (NOD; also known as the NACHT domain), and a C-terminal leucine-rich repeat (LRR) domain (Franchi, Warner, Viani & Nuñez, 2009). An inflammasome complex is set off when the pyrin domain of NLRP3 interrelates with the pyrin domain of ASC (Vajjhala, Mirams & Hill, 2012). The NOD domain contains ATPase activity needed for NLRP3 oligomerization which in turn results in NLRP3 inflammasome activation (Duncan et al., 2007). There are controversies about the mechanism of the NLRP3 inflammasome, however, two signalling methods (priming and activation) have been proposed (Lamkanfi & Kanneganti, 2010).

NLRP3 Stimulation – priming and activation

A two way-signal mechanism has been suggested for NLRP3 inflammasome activation and neither of the signals alone does activate the NLRP3 inflammasome (Juliana et al., 2012; Lopez-Castejon et al., 2012). The first signal (priming) is propagated by microbial elements or endogenous cytokines, which stimulate the NLRP3 inflammasome. The second signal (activation) of the NLRP3 inflammasome stems from extracellular Adenosine Triphosphate (ATP), pore-forming toxins, or particulate matter (Juliana et al., 2012). In the priming step of NLRP3 activation, the microbes, such as lipopolysaccharide (LPS), engage in the transcription of NLRP3 by upregulating NLRP3 and cytokines (see Figure 1). The transcription and upregulation of NLRP3 induced by priming leads to a vigorous inflammatory response (Bauernfeind et al., 2009). Since NLRP3 is ubiquitinated in the LRR domain, the priming of NLRP3 triggers deubiquitinating enzyme (BRCC36) which then deubiquitinates NLRP3 (Shi et al., 2015).

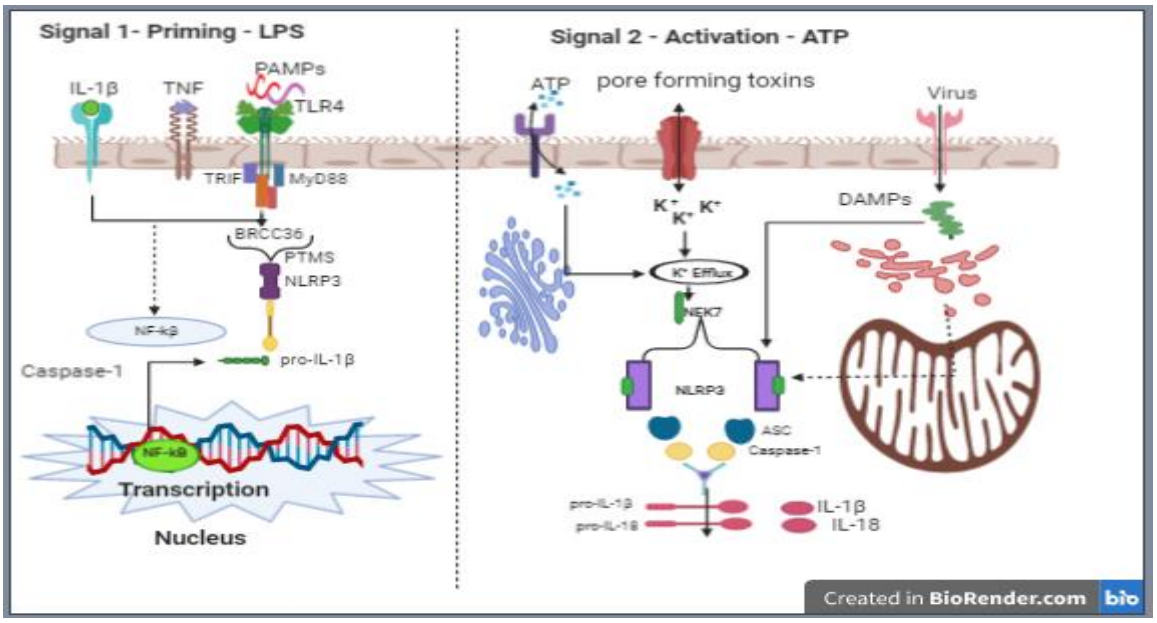

Figure 1. A figurative representation of NLRP3 inflammasome activation**,** showing a bipartite signal model. The priming signal 1 (left side) is induced by microbial organisms (LPS) and signal 2 (right side) is induced

by endogenous elements (ATP), leading to the activation of the transcription factor and subsequent activation of NLRP3 and cytokines. This Figure is inspired by Kelley et al (2019).

The toll-like receptor 4 (TLR4), as seen in Figure 1, is a member of the TLRs family, which is critical for recognizing lipopolysaccharide (LPS) and for activation of innate immunity, which subsequently leads to the production of pro-inflammatory cytokines and chemokines (Vaure & Liu, 2014). The activation of TLR4 triggers two signalling pathways: the MyD88 and the TRIF signalling pathways. Both pathways form a complex that regulates NF-κB, which then activates NLRP3 and subsequently stimulates pro-IL-β and pro-IL-18 (Kelley et al., 2019).

NEK7-NLRP3 Interaction

Never in mitosis A-related kinase 7 (NEK7) or, short name, NimA-related protein kinase 7 (NEK7), is a major protein that regulates the mitotic mechanism (Yissachar, Salem, Tennenbaum, & Motro, 2006). It engages in chromatin condensation by phosphorylating histone (H3) and engages in the reformation of the microtuble network in the mitotic process (Yissachar, Salem, Tennenbaum, & Motro, 2006). More so, NEK7 can biologically be found at the centrosome all over the cell cycle, functions in the centrosome and is monumentally crucial in spindle formation at prometaphase and cytokinesis during mitosis (Kim, Lee, & Rhee, 2007).

Most importantly, a study has shown that NEK7 is one of the vital elements of the NLRP3 inflammasome in macrophages (Zhou et al., 2016) (Figure 1). A research was done on mice to investigate the effect of NEK7 on inflammatory bowel disease (IBD), which is rampant among mutant inflammation-associated conditions in the gastrointestinal tract (Chen et al., 2019). Interestingly, Chen t al (2019) described that NEK7 interacts with NLRP3 to facilitate the inflammasome activation and cell pyroptosis, hence hindering the IBD advancement. According to Chen, Liu, Yuan, et al (2019), the dysregulation of NEK7 induces an interruption of the cell's homeostasis, which leads to abnormal cell growth. It was seen that the NEK7 knockout immensely triggered the reduction of NLRP3 and IL-1β. Chen et al (2019) conducted this experiment using small interfering RNA (siRNA) to investigate the role of NEK7 in the activation of the NLRP3 inflammasome.

CRISPR/Cas9 System

Clustered regularly interspaced palindromic repeats (CRISPR)/Cas9 is a modern gene editing technique used in biomedical research (Redman, King, Watson, & King, 2016). The CRISPR/Cas9 facilitates the possibility of correcting errors in the genome and in a quick, cheap, and reasonably easy way turn on or off genes in cells and organisms. It has a lot of biological applications including rapid creation of cellular and animal models, functional genomic screens, and live imaging of cellular genome. It is widely used in clinical applications, such as gene therapy, and the treatment of infectious diseases (Redman, King, Watson, & King, 2016).

The CRISPRs are the repeated segments of DNA originally found in prokaryotic organisms. CRISPR and CRISPR-associated (Cas) proteins are among the adaptive immune systems in archaea and bacteria which defend against invasive microbial organisms (Liu, Zhang, Liu, & Cheng, 2017). CRISPR was first discovered in Japan, at the Osaka University, by Ishino in 1987 (Ishino, Shingawa, Makino, Amemura & Nakata, 1987). After numerous structural similarities were found in different bacteria and archaea, Janson proposed the acronym (CRISPR) in 2002 and in 2005 Mojica and associates speculated that CRISPR and its related proteins have immune defense functions (Liu, Zhang, Liu, & Cheng, 2017).

Cas proteins are endonucleases which use a single guide RNA (sgRNA) to create a complementary base pair with target DNA and then cut the DNA at a specific site of interest. Among Cas proteins, Cas-9 is the mostly used (Figure 2). In gene editing, sgRNA recognizes the sequence of interest

while Cas9 protein cleaves it at a specific site of interest. The CRISPR/Cas9 system has two pathways: The Non-Homologous End Joining (NHEJ) repair pathway and the Homology Directed Repair (HDR) pathway. The NHEJ repair pathway repairs the double strand breaks (DSBs) by generating insertion or deletion (InDel), which leads to frameshifts and/or premature stop codon. Contrarily, a donor DNA template is required to repair the DSBs in the HDR Pathway (Liu, Zhang, Liu, & Cheng, 2017).

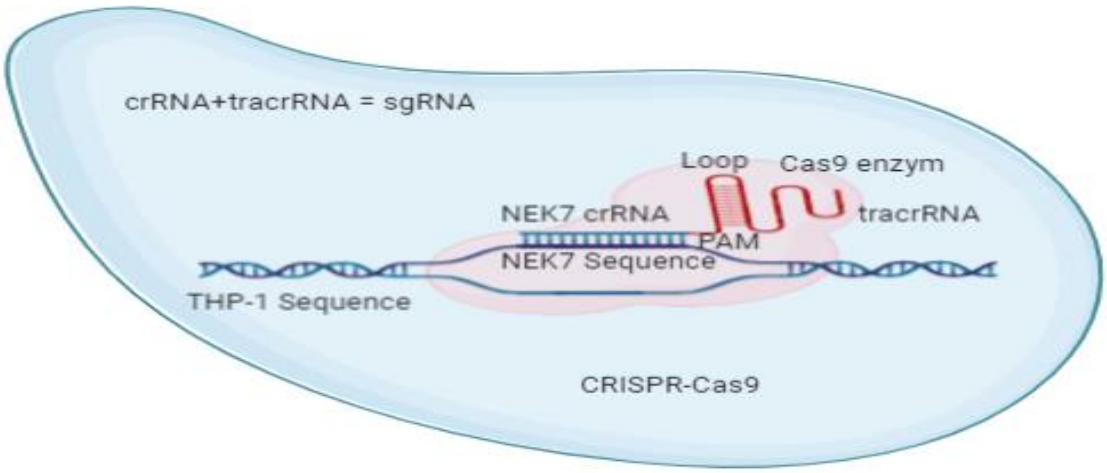

Figure 2. A genetical strategy to edit NEK7 protein using the CRISPR/Cas9 system. Firstly, a crRNA has a 20-nt complementary to the gene of interest upstream PAM sequence. The tracrRNA guides crRNA to locate the site of interest (20-nt NEK7), the enzyme (Cas9) cuts the gene of interest at 3 sequence upstream PAM sequence. These components form CRISPR/Cas9 (sgRNA). Figure 2 is inspired by Liu, Zhang, Liu & Cheng (2017).

This thesis project is aimed at using CRISPR/Cas9 technology to determine the intracellular effect of the NEK7 protein in the activation of the NLRP3 inflammasome in mammalian cells (THP-1) when knocked out. The main objectives are making a CRISPR/Cas9 construct and using this mechanism to investigate the role of NEK7 protein in the activation of NLRP3. In human THP-1 cells, a portion of NEK7 DNA sequence (24 base pair), which is the target, is to be cleaved using CRISPR/Cas9 mechanism and subsequently repaired by the NHEJ repair pathway. In the previous experiment conducted by Chen et al (2019), NEK7 was silenced in a mouse intestinal epithelia cell line but in this experiment, mammalian cells will be used to investigate the role of NEK7 as it relates to the activation of NLRP3 inflammasome. Hypothetically, NEK7 knockout will lead to reduction in the NLRP3 inflammasome's activation, and in IL-1β and IL-18 formation.

Materials and methods

Construction of forward and reverse oligonucleotides

The oligo 1 (forward primer) and oligo 2 (reverse primer) of "Never in mitosis A-related Kinase 7" (NEK7) were constructed using the Benchling software, supplied by Invitrogen. The purpose of the oligos (24 base pairs (bp)) was to create a sequence that is complementary to the portion of the targeted NEK7 DNA sequence (24 bp) and ligate it in a pGuide-it Vector (approximately 8 kb) and then transform it into *stellar* competent cells (Clontech Laboratories, Inc.). The control oligos (scrambled sequences that do not recognize any genes) were also provided by the company (Clontech). According to the Guide-it™ CRISPR/Cas9 protocol, this construct was transfected into THP-1 cells, where the annealed oligos located the portion of the targeted DNA (24 bp) and were

expected to knock it out (Clontech). The parameters, e.g. GC contents, were analyzed using Oligo Analyzer (Integrated DNA Technology) The oligos designed can be found in Figure 3.

Figure 3. Showing the 20 bp target sequence with the 3 PAM sequence in blue colour at the 3´end. The PAM sequence guided the sgRNA to where to cut, most often 3 sequences upstream the PAM sequence. Oligo 1 and 2 contained overhangs in red sequences, which were created to match the overhangs of the vector to ensure an optimal ligation.

Cloning

The oligos 1 and 2 of NEK7 and control oligos 1 and 2, the latter consisting of scrambled sequences, were annealed according to the Guide-it™ protocol by mixing oligo 1 and 2, Guide-it oligo, and annealing Buffer (Clontech). The oligos' mixture was then annealed using a thermal cycler (Biometra) to denature at 95^0 C for 2 minutes and reanneal at a 85^0 C to 30^0 C slope for approximately 10 minutes (Clontech).

According to the protocol (Clontech), the annealed oligos (target oligos and control oligos) were cloned into the pGuide-it Vector (Clontech). The reaction mix was incubated at 22^0 C for 7 minutes instead of 16^0 C for 30 minutes as instructed by the protocol – because the room temperature was higher than 16^0 C, the time had to be reduced – and the mix was then transformed into s*tellar* competent cells following the protocol instructions (Clontech).

The LB-agar + ampicillin plates and non-ampicillin plates were pre-warmed at 37^0 C for approximately 30 minutes and the recombinant DNA was plated in different volumes (5, 10, 20, 40, 60, 80, 100, 150, 200 and 250 µl) and incubated overnight at 37^0 C. After overnight incubation, four colonies were selected, suspended in 5 ml LB-Broth + ampicillin (100 µg/ml) and incubated overnight at 37^0 C. Plating was also done according to the LB-agar plates Addgene protocol recommendations (Addgene).

The four selected colonies were purified using QIAprep® Spin Miniprep Kit (QIAGEN). According to the protocol, QIAprep® Spin Miniprep Kit (QIAGEN), the colonies in 5 ml media were centrifuged at 8000 rpm (6800 x g) for 3 minutes using a multi-purpose centrifuge – ScanSpeed 1580 MGR (LABOGENE). LyseBlue reagent was not added in the process and the DNA was eluted with 50 µl Buffer EB according to the protocol (QIAGEN). Futhermore, the purities and concentrations were measured using Nanodrop (Themo Fisher) and Qubit (Thermo Fisher) respectively. Two samples, named 1c and 4c, were sent for sequencing according to the KIGene guidelines and the Guide-it™ sequence primer 1 (5'- AATGGACTATCATATGCTTACCGT-3') was used for sequencing as recommended by the pGuide-it Vector protocol (Clontech).

Cells culturing and transfection

THP-1-ASC-GFP cells (Invivogen) were cultured using the cells' media components. That include; 2 mM RPMI 1640 w.L-glutamine (Sigma) , 10 % heat inactivated FBS (Sigma), 100 mM sodium pyruvate (Sigma), 0.45 % glucose solution (Sigma), 1 M HEPES (Sigma) and 100 U/ml pen-strep (Sigma-Aldrich). The cells were incubated with a 5 % CO_2 incubator (SANYO) at 37^0 C. Additionally, the cells were counted every second day by mixing 100 µl of trypan blue (Sigma-

Aldrich) and 100 µl of the culture media, after which 10 µl of the mix was counted using an optical microscope (VWR). The cells' media was changed every second day by centrifuging the cells culture at 1000rpm for 5 minutes. The supernetant was discarded and the pellet was resuspended in a fresh media. The cells' density was kept between $5x10^5$ and $1.5x10^6$ cells/ml using this formula:

Number of cells/2 * 10000 = cells/ml

Cells/ml * volume of cells media = Total cells

Cells density (between 5 $x10^5$ and $1.5x10^6$ cells/ml cells) = total cells/500 cells/ml.

Sample 4c was transfected into THP-1 cells using ViaFect™ Transfection Reagent (Promega). 24-well plate was used, however, 18-wells were plated. The transfection was performed according to the prototocol as shown in Table 1. The ViaFect™ transfection reagent was mixed with 0.5 µg of plasmid DNA and diluted with a serum- and antibiotic-free media, then incubated for 20 minutes at room temperature as instructed in the protocol (Promega).

Table 1. Transfection components

Plate size	Cells/well	Volume of cells in media/well	Transfection complex/well	Amount of DNA/well	Reagent/well	Ratio
24-well plate	200,000	450 µl	50 µl	0.5 µg	2 µl	4:1

The transfection was performed in three parts; non-transfected, transfected and transfected control. 10 ng/ml of para-Methowyamphetamine (PMA) (Invivogen) was used to differentiate the cells for 4 hours. Each of the three parts underwent three conditions; 1. Un-prime, 2. Prime and 3. Prime and Activation condition. The cells were stimulated with 200 ng/ml Lipopolysaccharides (LPS) (Invivogen) for 4 hours then activated with 5 nM Adenosine Triphosphate (ATP) (Sigma) for 30 minutes. The Total RNA Purification Kit (NORGEN) was used to extract 9 RNA samples. The cells' media was aspirated and the monolayer cells were washed with 600 µl PBS according to the protocol (NORGEN). Following the protocol, The Total RNA Purification Kit (NORGEN), 200 µl of 100 % ethanol was used to lysate the cells, which were then eluted with 50 µl of Elution Solution A at 14,000 x g (14,000 RPM). Nanodrop (Thermo Fisher) and Qubit (Thermo Fisher) were used to measure the absorbance values (purities) and the concentrations of the RNA samples. Total RNA extraction (NORGEN) was used to extract RNA since the next step in this study was conversion of RNA to cDNA for the purpose of a qPCR run.

qPCR and reverse transcription

The High-Capacity RNA-to-cDNA™ Kit (Applied Biosystems) was used to convert RNA samples to cDNA using 2X RT Buffer Mix, 20X RT Enzyme Mix and RNA samples (19.8 ng/20 µl). Following the High-Capacity RNA-to-cDNA™ instructions, a thermal cycler (Biometra) was used to incubate the reaction at 37^0 C for 60 minutes, then stop the reaction by heating at 95^0 C for 5 minutes and hold at 4^0 C, following Applied Biosystems' instructions. The NEK7 oligos (FP 5'- ATT TGG GCC ACT CTG TAT GC -3', RP 5'- GGC TGT AGT CAT GGC CAG TT -3') and ACTB reference gene primers (FP 5´-CACCATTGGCAATGAGCGGTTC-3´, RP 5´- AGGTCTTTGCGGATGTCCACGT-3´) were designed using "Primer 3 plus" software.

The qPCR preparation was done according to the SYBR® Select Master Mix protocol (Applied Biosystems). Both oligos of the gene of interest (NEK7) and the reference gene (ACTB) had a concentration of 150 nM while the cDNA had 2 ng in a 10 µl reaction. There were 9 cDNA samples and each sample had a triplicate both in the NEK7 and in the ACTB oligos. Six Non-template control (NTC) samples were included. A qPCR 16 by 6 96-well plate containing samples was run on the qPCR machine (Thermo Fisher) according to the SYBR® Select Master Mix protocol (Applied Biosystems). The thermal cycling conditions were: An initial activation step for 2 min at 50° C, a denaturation step for 10 min at 95° C, then 40 cycles of 15 sec at 95° C, and extended for 1 min at 60° C. When analysing the qPCR data, the standard rules such as SD ≤ ±0.25 were considered (Institute for Research in Immunology and Cancer (IRIC), 2020). The statistically significant p-value was < 0.05 and the biological relevance threshold was set at ±1.5-log2 fold change in this thesis project study, which is consistent with the study conducted by Akond, Alam and Mollah (2018).

Ethics

Having gone through the WMA declaration of Helsinki – Ethical Principles for medical research involving human subjects, it has been found that this study is not bound by any ethical considerations therein (World Medical Association, 2018). The human THP-1 cells used in this study were done in vitro, therefore exempt from seeking consent and permission from authorities. However, to avoid environmental risk, waste from the human THP-1 cells were disposed of in biohazard waste. Furthermore, an environmental analysis was conducted in preparation for this study. Therefore, all the highly risk chemicals and waste, such as RNAse A, were disposed of in biohazard waste. Additionally, fume hood and fume sterile were used when necessary to avoid environmental pollution. Furthermore, the lentivirus vector method of transfection, which would have been the ultimate option for this study, was not used, since University of Skövde does not have the bio-safety classification required.

Results

DNA purity and concentration

There were bacterial colonies on the expected plates and none on the negative control plates (see Figure 1 in the appendix section). The four colonies selected were incubated at 37^0 C overnight, then the recombinant DNA was purified and measured. The Nanodrop spectrometer was used to measure the absorbance values (purity) of $A_{260/230}$ and $A_{260/280}$ wavelengths of the samples. Qubit was used to measure the concentration of the samples. The results obtained from the various samples can be seen in table 2.

Table 2. Purity and concentration of samples.

Sample	Nanodrop (Purity) $A_{260/230}$	Nanodrop (Purity) $A_{260/280}$	Nanodrop (Conc.) ng/ µl	Qubit (Conc.) ng/ µl
IC	2.85	1.95	191.5	163
2C	4.08	1.91	107.5	76
3C	3.24	1.92	154.2	72
4C	2.69	1.90	289.0	189

Verification of oligos

It was very crucial to know if the ligation worked, because the annealed oligos were part of the construct (sgRNA), which guides Cas9 to the target (NEK7 24 nucleotides) and Cas9 was expected to cut the target. The oligos designed in the methods section were annealed and ligated into vector, then cloned into *stellar* competent cells to form recombinant plasmid DNAs. Two recombinant plasmid DNAs were selected and sent for Sanger sequencing (KIGene Karolinska Institutet, Stockholm) to verify if the oligos (both NEK7 and control oligos) were successfully cloned into the pGuide-it Vector. According to the KIGene guidelines, the amount of sample suitable for sequencing is between 150ng-300ng in approximately 7µl (KIGene). In order to satisfy this requirement, the samples were measured not only to know the concentrations of the DNA samples but also to know the purities (Table 2). Since the nucleotides in Figure 4 and 5 are single strand DNA, only the oligo 1 (5'- GAAGGCCTTACGACCGGATA-3') was confirmed in both sample 1c and 4c, as indicated in blue color sequences in Figure 4 and 5, using the Finch TV software. Also, the oligo 1 of the control is represented in Figure 6 in blue color sequences (5′–TGACATCAATTATTATACAT-3′).

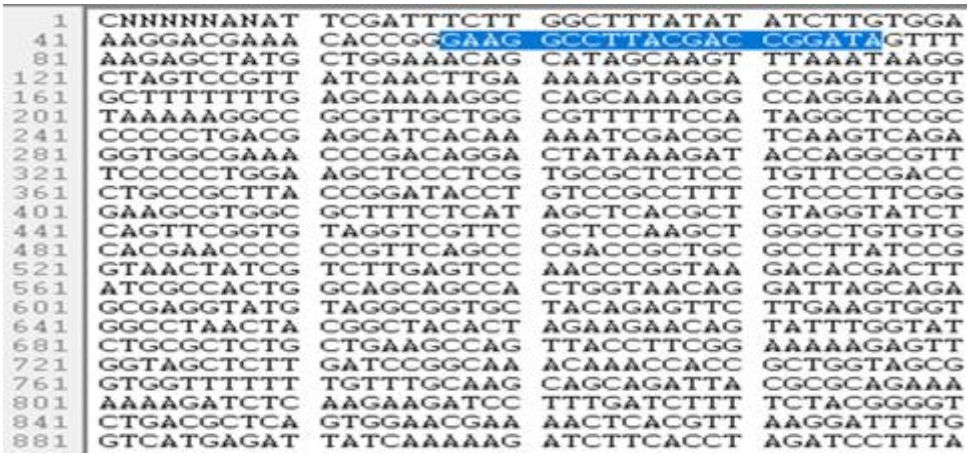

Figure 4. The sequence in blue colour shows that oligo 1 was optimally ligated into the vector in sample 1c of the recombinant plasmid DNA.

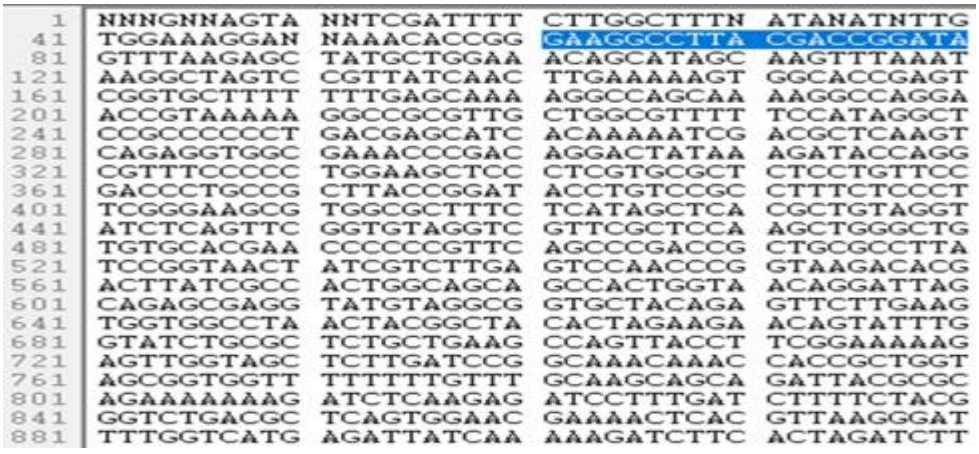

Figure 5. The sequence in blue colour shows that oligo 1 was optimally ligated into the vector in sample 4c of the recombinant plasmid DNA.

Figure 6. Sample c (control oligo 1) of the recombinant plasmid DNA with blue color sequence representing the oligo 1 of the control.

Transfection

Nine samples as shown in Table 3 were transfected and exposed to different treatments. All the samples were differentiated with PAM for 4 hours, six samples were stimulated by priming them with LPS for 4 hours and three samples were activated with ATP for 30 minutes. The monolayer cells were purified and the RNAs were measured after purification to ascertain the purities and the concentrations before performing reverse transcription. The results obtained can be found in table 3.

Table 3. RNAs purities and concentrations.

Sample	Nanodrop $A_{260/230}$	Nanodrop $A_{260/280}$	Nanodrop (Conc.) ng/ µl	Qubit (Conc.) ng/ µl
Non-transfected and Un-primed (NU)	0.32	2.06	11.2	6.78
Non-transfected and Primed (NP)	0.23	1.79	8.0	4.4
Non-transfected, Primed and Activated (NPA)	0.67	2.20	14.6	11.2
Transfected and Un-primed (TU)	0.60	1.96	13.4	10.8
Transfected and Primed (TP)	0.57	1.55	126.3	10.7
Transfected, Primed and Activated (TPA)	0.42	1.71	22.1	4.00
Control transfected and Un-primed (CU)	0.27	1.55	9.9	8.62
Control transfected and Primed (CP)	0.37	2.09	6.0	5.82
Control transfected, Primed and Activated (CPA)	0.03	2.47	6.7	2.20

qPCR results

In order to verify if the transfection was successful, qPCR was performed to determine the differences of NEK7 mRNA expression between non-transfected, transfected and control-transfected variables in different conditions [Un-primed (U), Primed (P) and Primed & Activated (PA)]. In Figures 7-13, the differences between the variables in different conditions are

investigated, by means of the Log2 fold change (having the calibrator at a value of 0) (Tilevik, A., (n.d.)). See Figure 2 in the appendix section for qPCR raw data.

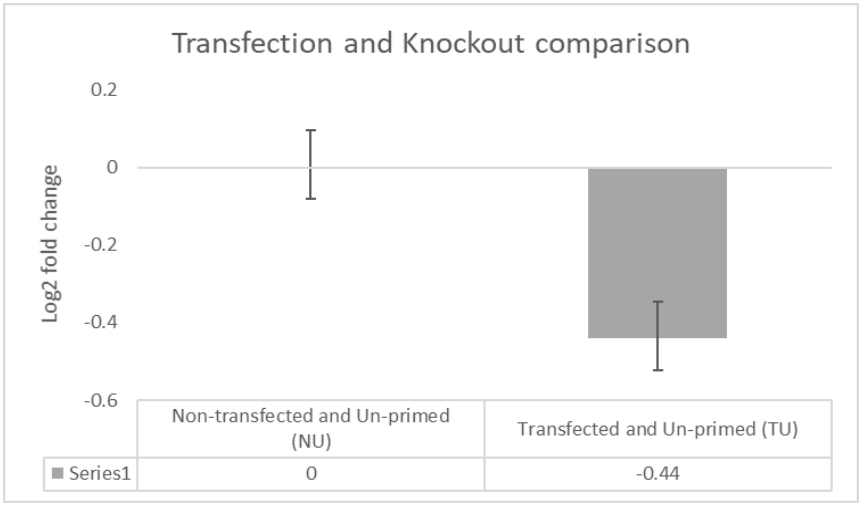

Figure 7. Comparison of NEK7 mRNA expression in Non-transfected and Un-primed (NU) cells with standard deviation ±0.09 (SD ±0.09) to Transfected and Un-primed (TU) cells (SD ±0.08). The sample NU serves as a calibrator (control) in this investigation, while sample TU was transfected with a portion of NEK7 DNA, which is the target. The value of each sample (NU and TU respectively) is an average of technical triplicates and both samples (NU and TU) were differentiated with PMA for 4 hours.

From figure 7, it could be seen that the Transfected and Un-primed (TU) sample shows a -0.4-downregulation of NEK7 mRNA expression compared to the Non-transfected and Un-primed (NU) sample, which shows a slight decrease of NEK7 mRNA expression in the TU sample compared to the NU sample. The TU sample represents THP-1 cells in which a portion of NEK7 nucleotide was intended to knockout using CRISPR/Cas9.

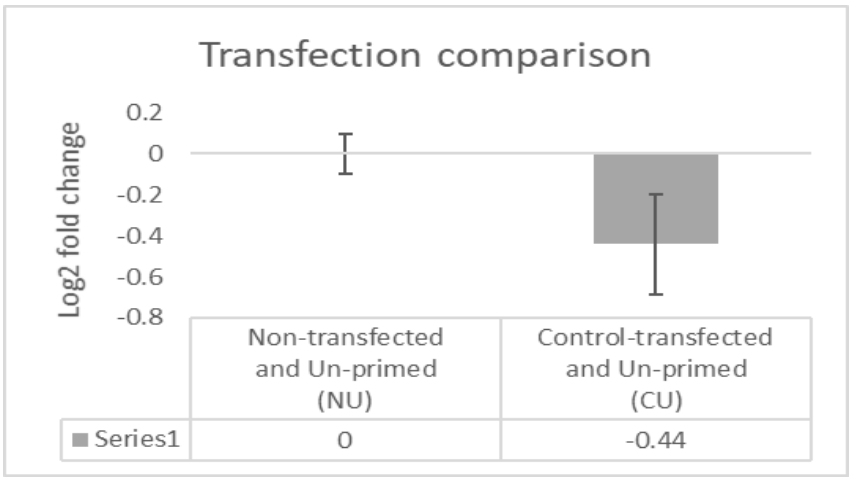

Figure 8. Comparing NEK7 mRNA expression in Non-transfected and Un-primed (NU) cells (SD ±0.09) to Control-transfected and Un-primed (CU) cells (SD ±0.25). In Figure 6, the NU sample contained wild-type THP-1 cells while sample CU represents cells with a control vector which does not target any sequences. The value of each sample (NU and CU) is an average of technical triplicates and both samples (NU and CU) were differentiated with PMA for 4 hours.

From figure 8, the Control-transfected and Un-primed (CU) sample constituted cells containing plasmid DNA with oligos that do not target any sequences, otherwise known as control plasmid,

which means it should not have an effect on THP-1 cells when knocked out, however, the CU sample indicates a -0.4 downregulation of NEK7 mRNA expression compared to the NU sample, hence, mRNA expression of NEK7 is decreased compared to the NU sample.

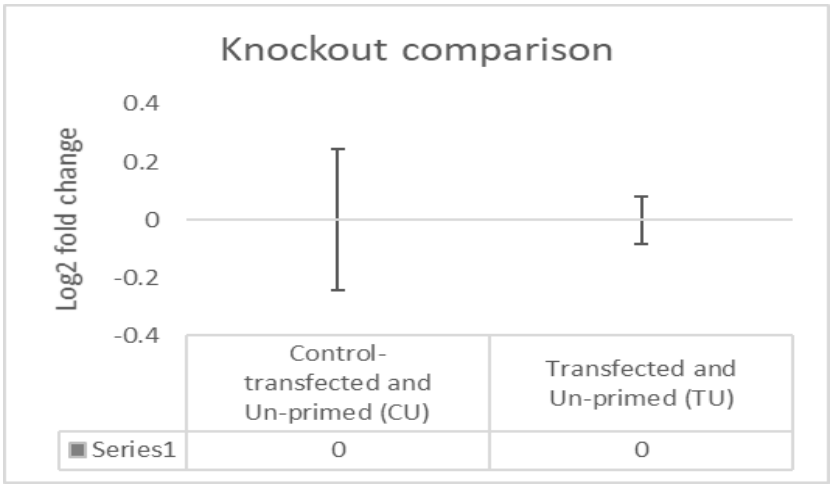

Figure 9. To compare mRNA expression in Control- transfected and Un-primed (CU) cells (SD ±0.25) to Transfected and Un-primed (TU) cells (SD ±0.08). The value of each sample (CU and TU) is an average of technical triplicates and both samples (CU and TU) were differentiated with PMA for 4 hours.

In sample CU, the annealed control oligos target no gene sequences in the THP-1 cells while in sample TU, the annealed NEK7 oligos in sgRNA target to knockout a portion of NEK7 DNA in the THP-1 cells. From figure 9, the TU sample shows an equal mRNA expression of NEK7 with the CU sample, which indicates no difference of NEK7 mRNA expression in both samples (TU sample and CU sample).

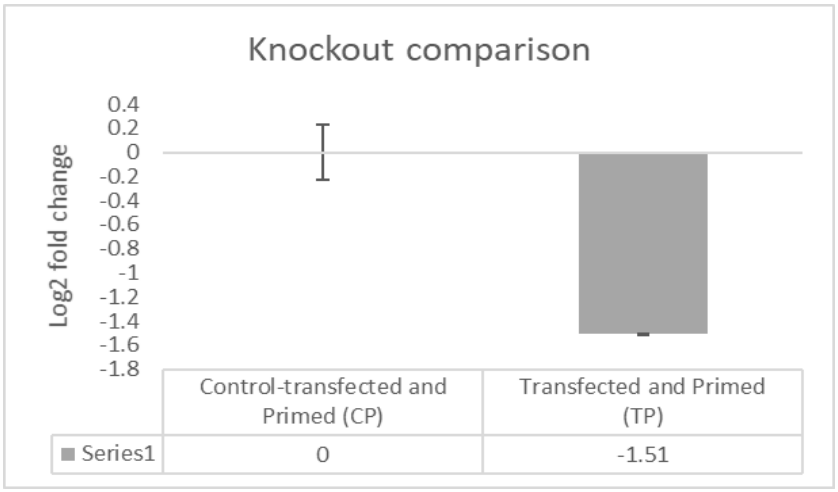

Figure 10. A comparison of NEK7 mRNA expression in Control-transfected and Primed (CP) cells (SD ±0.23) to Transfected and Primed (TP) cells (SD ±0.01). The value of each sample (CP and TP) is an average of technical triplicates and both samples (CP and TP) were differentiated with PMA for 4 hours and then stimulated by priming them with LPS for 4 hours.

In figure 10, it could be seen that the Transfected and Primed (TP) sample shows a -1.51 downregulation of NEK7 mRNA expression compared to the Control-transfected and Primed (CP) sample, therefore suggesting a decrease of NEK7 mRNA expression in the TP sample compared to the CP sample.

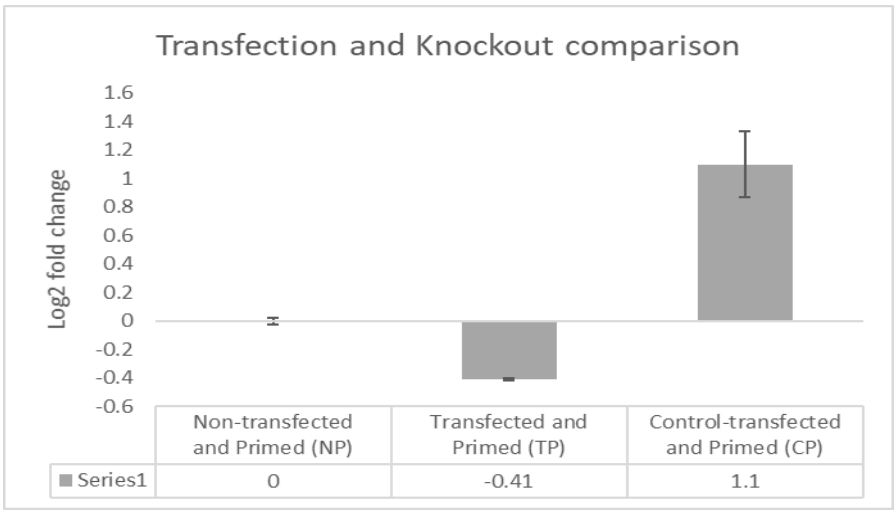

Figure 11. The NEK7 mRNA expression comparison in Non-transfected and Primed (NP) cells (SD ±0.02) to Transfected and Primed (TP) cells (SD ±0.01) and Control-transfected and Primed (CP) cells (SD ±0.23). The value of each sample (NP, TP, and CP) is an average of technical triplicates and the three samples were differentiated with PMA for 4 hours and then stimulated by priming them with LPS for 4 hours.

From figure 11, in sample TP, one can observe a slight (-0.4) downregulation of NEK7 mRNA expression in the THP-1 cells compared to the Non-transfected and Primed (NP) sample. However, sample CP shows a 1.1 upregulation of NEK7 mRNA expression in THP-1 cells compared to sample NP. Note that sample CP is a control for the knockout while sample NP is a control for the cells' viability.

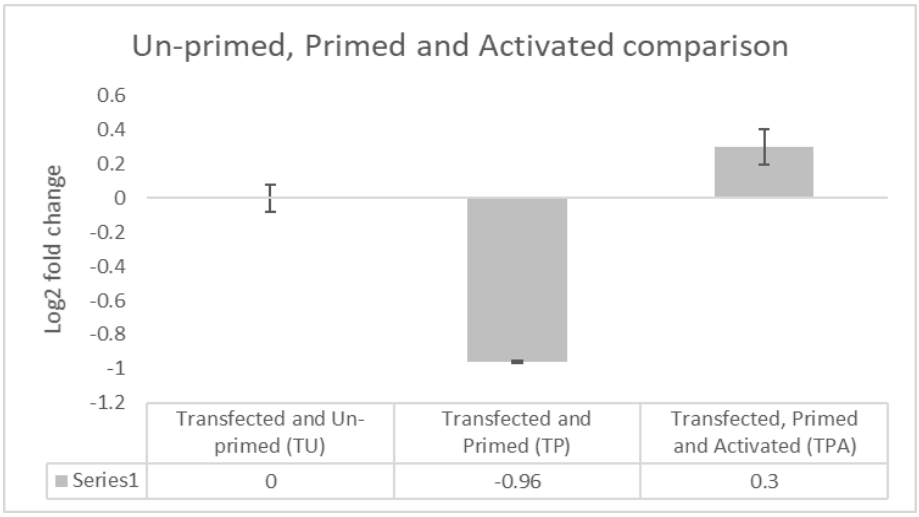

Figure 12. The comparison of NEK7 mRNA expression between the Transfected and Un-primed (TU) cells (SD ±0.08) to the Transfected and Primed (TP) cells (SD ±0.01) and Transfected, Primed and Activated (TPA) cells (SD ±0.11). The value of each sample (TU, TP and TPA) is an average of technical triplicates and the three samples were differentiated with PMA for 4 hours, but sample TP and TPA were then primed with LPS for 4 hours, while only sample TPA was activated with ATP for 30 minutes.

From Figure 12, it appears that sample TP indicates approximately a -1.0 downregulation of NEK7 mRNA expression in THP-1 cells compared to sample TU. The Transfected, Primed and Activated (TPA) sample suggests a 0.3 upregulation of NEK7 mRNA expression compared to sample TU, indicating an increase of NEK7 mRNA expression in THP-1 cells compared to sample TU.

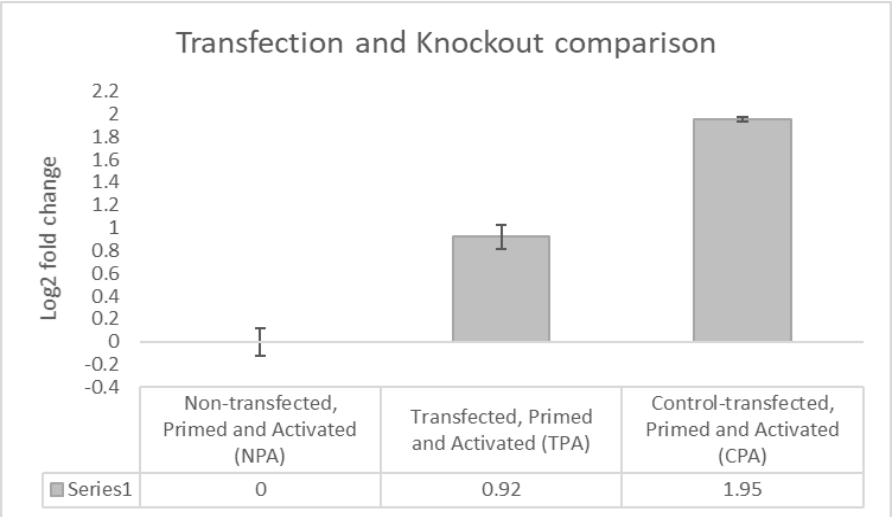

Figure 13. Figure 13 is a comparison of NEK7 mRNA expression in Non-transfected, Primed, and Activated (NPA) cells (SD ±0.12) to Transfected, Primed and Activated (TPA) cells (SD ±0.11) and Control-transfected, Primed and Activated (CPA) cells (SD ±0.02). The value of each sample (NPA, TPA and CPA) is an average of technical triplicates. The three samples in Figure 11 (NPA, TPA and CPA) underwent 4 hours differentiation with PMA, 4 hours LPS-stimulation and 30 minutes activation with ATP.

In figure 13, sample TPA shows a 0.9 upregulation of NEK7 mRNA expression compared to the Non-transfected, Primed and Activated (NPA) sample, suggesting an increase of NEK7 mRNA expression in sample TPA compared to sample NPA. Additionally, sample CPA shows a 1.9 upregulation of NEK7 mRNA expression in THP-1 cells compared to both sample NPA and TPA, indicating an increase of NEK7 mRNA expression. Since the data obtained were few, not up to 30, and the data were not normally distributed, the Kruskal-Wallis test, a non-parametric test, was used to investigate if the differences between the samples were statistically significant (p-value = 0.05). Statistical tests of Figure 7 to Figure 13 were performed but none was statistically significant, for example, the p-value of the samples in Figure 13 was 0.368.

Discussion

The aim of this study was to investigate the role of NEK7 protein in NLRP3 inflammasome activation. In achieving this goal, two main objectives were taken into consideration, i.e. to make a CRISPR/Cas9 system construct for NEK7 protein and to investigate if NEK7 knockout is successful in THP-1 cells. The methodology was to knockout the NEK7 DNA from THP-1 human cells and verify the knockout with qPCR technique by examining the NEK7 mRNA expression between the non-transfected cells, control-transfected cells, and the transfected cells. The hypothesis is that the NEK7 interaction with NLRP3 induces NLRP3 inflammasome activation, therefore, if NLRP3 inflammasome was activated by NEK7, it would emit cytokines such as IL-18 and IL-1β. On the contrary, if NEK7 were knocked out, the activation of the NLRP3 inflammasome would be insufficient, which leads to less emission of IL-18 and IL-1β. This assumption is in line with a previous study conducted to investigate the effect of NEK7-NLRP3 interactions on pyroptosis in inflammatory bowel disease via NF-κB signalling (Chen, Liu, Yuan et al., 2019). Chen et al (2019) concluded that NEK7 is essential in the activation of NLRP3 inflammasome and the knockout of NEK7 results to the blockage of the development of inflammatory bowel disease.

The plasmid DNAs (sample 1c and sample 4c) would not have been sent for sequencing if their purities and concentrations were not satisfactory. According to KIGene guidelines, the amount of

sample suitable for sequencing is between 150 ng - 300 ng in approximately 7 µl (KIGene). To satisfy this requirement, the samples were measured not only to know the concentrations of the DNA samples but also to know the purities. At this step of this study, if the concentrations and the purities were below expectation, the experiment would have stopped, and the process of DNA purification would have been repeated.

As shown in Figure 4, 5 and 6 in the Results section, the sequencing indicates that the annealed oligos were properly ligated into the Guide-it™ Vector. The sequences marked in blue colours represent the oligos. The sequencing mechanism is crucial to verify if the oligos were ligated to the vector or not. Since the oligos in Figure 4 and 5 were part of the sgRNA that guides Cas9 to the site where Cas9 was expected to digest, it is then extremely critical to ensure that the oligos were adequately ligated. Otherwise the whole experiment would have been an exercise in futility. Figure 6 contained a control oligo 1 in blue colour, which targets no sequences and was used to compare to NEK7 oligos in order to know if the NEK7 DNA knockout worked.

The DNA sequencing is a vital technique used widely in life science for verification purposes. For example, had it been that the transfection worked, NEK7 DNA sequencing would have been performed to investigate if the CRISPR-technique had worked. Two samples containing 24 bp of NEK7 DNA would have been sent to Karolinska Institutet for sequencing, and the Finch TV software would have been used to verify if the CRISPR/Cas9 mechanism digested the target. This mechanism of verification is consistent with previous studies (González, Shaimar, Liu, Blankenship, & Zhu, 2020). For example, González, Shaimar, Liu, Blankenship and Zhu (2020) investigated whether the ptchd3 gene has an effect in the mouse spermatogenesis and sperm function. The sequencing technique was used in their investigation to compare the sequence of the wild-type testis to the sequence of the mutated testis. The comparison proved that the sequence of the mutated testis had increased by approximately 115 bp.

In Table 2, the absorbance values of $A_{260/280}$ obtained were within the standard acceptable values (1.8 – 2.0). However, the absorbance values of $A_{260/230}$ were a bit higher than required, for example, sample 1c and 4c had absorbance values of 2.85 and 2.69 respectively, which was indicative of impurities. These impurities may have been a result of making blank measurements on a dirty pedestal and using blank solution that did not have the same components as the sample (Wilfinger, Mackey & Chomczynski, 1997). The standard acceptable $A_{260/230}$ absorbance value (2.0 – 2.2) was used to further determine the purity of the samples (Wilfinger et al., 1997). However, since the $A_{260/280}$ ratio was within the general acceptable values as in Table 2, the experiment continued. Table 3 shows values obtained from Nanodrop and Qubit of nine samples after transfection and RNA purification. It was crucial to determine the purities and the concentrations of the RNA samples before forging ahead. Most of the samples in Table 3 were within the general accepted values ($A_{260/280}$, 2.0 – 2.2) (Wilfinger et al., 1997). However, there were a few samples that indicated substandard values: Sample NP ($A_{260/280}$ = 1.79), TP ($A_{260/280}$ = 1.55), TPA ($A_{260/280}$ = 1.71) and sample CU ($A_{260/280}$ = 1.55). The low values could be due to contamination by DNA, protein, and unwanted organic compounds (Wilfinger et al., 1997; Olson & Morrow, 2012). Table 3 shows that the $A_{260/230}$ absorbance values were lower than the generally accepted values (2.0 – 2.2). The $A_{260/230}$ values for pure nucleic acid (DNA and RNA) are supposed to be higher than their corresponding $A_{260/280}$ values (Wilfinger et al., 1997). The low $A_{260/230}$ absorbance values shown in Table 3, could be because of residual protein and phenol during the nucleic acid purification (Wilfinger et al., 1997). Irrespective of the few substandard values, the experiment continued

because the values were relatively good, but it appears that the impurities may have contributed to less than optimal qPCR results.

Another important stage in this study was transfection, which is a technique in which nucleic acids are introduced into eukaryotic cells without viral methods (Groskreutz & Schenborn, 1997). Having considered some factors, such as cost, time and tools, liposomal transfection was used in this study. A liposomal system of transfection is a lipid bilayer form of delivering nucleic acids into eukaryotic cells (Sessa & Weissmann, 1968). Liposomal transfection is simple, convenient, less expensive and does not need sophisticated machines. An earlier study that is related to this study used liposomal transfection (He, Zeng, Yang, Motro, & Núñez, 2016). The analysis of He et al (2016) shows that NEK7 is a most important interacting associate of NLRP3.

In this thesis project, the recombinant plasmid DNAs were introduced into human THP-1 cells using ViaFect transfection reagent. After transfection, the cells were differentiated for 4 hours with para-Methoxyamphetamine (PMA), primed for 4 hours with Lipopolysaccharides (LPS) and activated for 30 minutes with Adenosine Triphosphate (ATP). The PMA was used to make the cells adherent to the plate, in other words, form monolayer cells. The reason to ensure that the cells adhered to the plate, was to avoid aspirating the cells together with the cells' media. This strategy is consistent with the previous study conducted by Park et al. (2007), where optimized THP-1 differentiation was required for the detection of responses to weak stimuli. The minor difference was that Park et al. (2007) differentiated with different concentrations (2.5 – 100 ng/ml) for 48 hours, while in this thesis project, the cells were at first stimulated by priming with 200 ng/ml LPS for 4 hours instead. It could have been that the 4 hours priming or stimulating time with LPS was not enough to activate the cells and may have affected the efficiency of the transfection and in turn affected the emission of pro-cytokines (e.g. pro-IL-18 and pro-IL-1β).

The priming induces NLRP3 protein which leads to the production of pro-cytokines (Bauernfeind et al., 2009). In this thesis project, if ELISA had been performed, the level of the pro-cytokines produced, especially IL-18, would have signified if NEK7 is critical for the activation of the NLRP3 inflammasome. This step was also taken in previous studies where cells were primed with LPS (Franchi, Eigenbrod, & Núñez, 2009; Sharif et al., 2019). Secondly, the cells were further stimulated by activating them with 5 mM ATP for 30 minutes. Cells are activated with ATP because LPS alone does not activate cells. Note that when cells are activated due to the invasion of PAMPs and DAMPs, NLRP3 protein is activated and oligomerized with other PRRs to form the NLRP3 inflammasome (Cai et al., 2014; Sborgi et al., 2015).

When analysing the qPCR data, the standard rules according to the Institute for Research in Immunology and Cancer (2020), such as including samples with a standard deviation lower than or equal to 0.25 (SD ≤ ±0.25), were adhered to. Hence, all the samples with a standard deviation greater than 0.25 were excluded. In Figure 2 in the appendix section, the numbers in red colour were SD values that were greater than 0.25 and therefore were excluded in the triplicates. Excel (Microsoft) was used to analyse the qPCR data. The parameters calculated with Excel were ΔCt (difference in cycle threshold), ΔΔCt (fold change), 2^-ΔΔCt (2-fold change) and Log2 fold change. Most of the triplicates had the same Ct values and the averages were calculated. In some triplicates, one sample differed from the other two samples. The differing sample was eliminated, and the average of the duplicate was calculated. The log2 fold change of the nine samples was used to determine the mRNA expression of NEK7 as indicated in Figures 7 to 13.

Even though Martínez-Abraín, (2008), says "Biological relevance is decided a priori (independently), and it is not necessarily a large value. You have to judge the magnitude you consider biologically relevant on a case by case basis", the biological relevance threshold in this thesis project was set at ±1.5-log2 fold change, which is consistent with the study conducted by Akond, Alam and Mollah (2018), where out of 401 differentially expressed genes identified in a HIV viremic vs avirmeic state real dataset, 28 differentially expressed genes were upregulated and 381 genes were downregulated applying a log2 fold change threshold value at ±1.5.

At this point, the core analysis of the fundamental result will be unveiled. In figure 7, it appears that sample TU (Transfected and Primed), was -0.4 downregulated of NEK7 expression compared to sample NU (Non-transfected and Un-primed), suggesting that transfection and gene editing may have had an effect to some extent on the THP-1 cells. This difference in the NEK7 mRNA expression in sample TU and NU, may have been because of the inconsistency in the values of the ACTB reference gene, though. In all circumstances, the downregulation was considerably below the threshold value.

In Figure 8, sample CU was -0.4 downregulated of NEK7 mRNA expression in THP-1 cells compared to the NEK7 mRNA expression in sample NU. This was not the expected result, because sample CU (Control-transfected and Un-primed) contained scrambled sequence oligos that do not target any gene sequences in THP-1 cells. The NEK7 mRNA expression level in sample CU should have equalled the NEK7 mRNA expression level in sample NU, but it was not equal, possibly due to the following factors. It could have been that the transfection disrupted the NEK7 mRNA expression, but the primary and supreme factor should be the poor stability of the ACTB reference gene. Since the ACTB reference gene had an equal amount of ACTB primer in all the samples, it was expected to have equal Ct values in all the samples (see raw qPCR data in Figure 2 in the appendix section) but there is a variation of Ct values, which in all probability has affected the corresponding samples during normalization.

This instability of ACTB in this thesis project is contrary to the result in the study conducted by Bustelo et al. (2020), on hypoxia and hypothermia in the neonatal rat brain, that the ACTB reference gene is among the most stable reference genes. The ACTB was used in this thesis project because most articles consider the ACTB reference gene highly stable for normalising monocytes (Cao et al. (2012). Contrary to Bustelo's et al. (2020) conclusion, a study conducted by Cao et al. (2012), where eight reference genes were used and the genes' stability were examined and listed from the most stable to the least stable, ACTB ranked second lowest among the eight reference genes: PGK1, GAPDH, PPIB, SDHA, RPL37A, TBP, HPRT1, PPIA, ACTB and RPL13A. Hence, Cao et al. (2012) concluded that ACTB is not reliable. However, both Bustelo et al. (2020) and Cao et al. (2012), were in agreement that series of studies have shown that the stability of a reference gene depends on the environmental conditions.

In Figure 9, there were no differences in NEK7 mRNA expression in sample TU compared to sample CU. The NEK7 mRNA expression of sample TU was expected to be downregulated compared to that of sample CU, if transfection and knockout had worked successfully. The overriding reason for this should be the variations in the Ct values of the ACTB reference gene. Sample CU was transfected with a control plasmid DNA, which targeted no genes, therefore, the knockout would not make any changes since the annealed oligos contained in the sample CU did not recognise any genes in the THP-1 cells.

Figure 10 represents the difference of NEK7 mRNA expression between sample TP and CP. Both samples were differentiated with PMA for 4 hours and then primed with LPS for 4 hours. The difference is that sample CP contained a control plasmid DNA, therefore did not recognize any gene sequences in the THP-1 cells. From Figure 10, it is observable that sample TP was -1.5 downregulated of NEK7 mRNA expression compared to sample CP, arguably because the target (NEK7) may have been knocked out from the human THP-1 cells using pGuide-it Vector CRISPR/Cas9. The -1.5 downregulation of NEK7 mRNA expression in sample TP compared to sample CP is in compliance with the biological relevance set for this thesis project (±1.5), however, considering the variations in the Ct values of the ACTB reference gene, this difference cannot be validated.

In Figure 11, sample NP, the calibrator with the value of zero, was compared to sample TP and CP. It appears that sample TP was -0.4 downregulated in terms of NEK7 mRNA expression compared to both sample NP and CP, while in sample CP, the NEK7 mRNA expression was 1.09 upregulated compared to sample NP. This was not the expected outcome, but this result could be due to impurities and most likely due to the ACTB instability. The upregulation of NEK7 mRNA expression in sample TPA in Figure 13 was also abnormal. The NEK7 mRNA expression of sample TPA was 0.9 upregulated compared to sample NPA, this may be due to instability of the ACTB reference gene, which was used to normalise the target (NEK7). Remarkably, Figure 13 reflects the main expected result in this thesis project study. Both sample TPA and CPA in the Figure 11 had the same treatment (Transfection, PMA-differentiation, LPS-Priming and ATP-Activation). The only difference between the samples was that sample TPA had annealed oligos that were complimentary to a portion of NEK7 DNA sequence in THP-1 cells. Figure 13 shows that sample TPA was 0.9 downregulated of NEK7 mRNA expression compared to sample CPA, but the difference could have been as the result of the ACTB inconsistency. Even so, the difference of NEK7 mRNA expression between the samples was not within the ±1.5-log2 fold change threshold.

Also, with the variations in the Ct values of the ACTB reference gene, one cannot say that the knockout was successful. As described in Figure 2, the CRISPR/Cas9 system, that consists of sgRNA and enzymatic nuclease (Cas9), was expected to use the sgRNA consisting of crRNA and tracrRNA, with crRNA containing a complementary DNA sequence specific to the NEK7 targeted DNA sequence. The tracrRNA was supposed to guide the Cas9 protein to cleave the NEK7 targeted DNA sequence 3 codons upstream the PAM sequence. The cleavage site was expected to be repaired by non-homologous end joint (NHEJ) DNA repair, which results in insertions/deletions (INDELs) mutations. Since the instability of the ACTB reference gene affected the NEK7 mRNA expression results, one cannot conclude that the CRISPR/Cas9 mechanism worked successfully in this thesis project.

The CRISPR/Cas9 editing mechanism used in this thesis project is different from a previous study related to this thesis project conducted by Chen, Liu, Yuan, et al (2019), where short interference RNA (siRNA) technique was used instead of CRISPR/Cas9 technique to knockout NEK7 targeted DNA in the investigation of how NEK7 interaction with NLRP3 could control the pyroptosis in inflammatory bowel disease via NF-κB signalling on MODE-K cells of mice. They used the same steps with a few exceptions, such as the use of virus as a vector. They verified the emission levels of proteins and cytokines with commercial ELISA and found that the "NEK7 knockout significantly decreased the protein levels of NLRP3, caspase-1 (p20), GSDMD-N, and the emission of IL-1β in MODE-K cells, signifying that NEK7 knockout could obstruct NLRP3 inflammasome's activation

and pyroptosis in vitro and concluded that NEK7 was a critical protein to inducing NLRP3 inflammasome's activation".

More so, previous related studies have not used the CRISPR/Cas9 system on human cells. Instead there are several studies that have used siRNA on mice/human and CRISPR/Cas9 on mice only (Kim, Lee & Rhee, 2007; Haq et al., 2015; Schmid-Burgk et al., 2015; Chen, Liu, Yuan, et al., 2019; Chen, Meng, Bi, et al., 2019). For example, in a study conducted by Chen, Meng, Bi., et al (2019), NEK7-shRNA virus was used in the NEK7 DNA knockout in primary cortical neurons in mouse. It was deduced that the NEK7 knockout resulted to the blockage of the activation of NLRP3 inflammasome after traumatic brain injury (TBI). Chen, Meng, Bi., et al (2019), stated that the knockout of NEK7 DNA contributed to the significant decrease in the mRNA expression of NLRP3, caspase-1, ASC, GSDMD and pro-IL-1β.

Liposomal transfection has several advantages. It is cheap, easy to access commercially, does not need sophisticated machines, is not necessarily time consuming, targets a specific region and guarantees safety. However, it has less efficiency, especially on the immune cells (THP-1), which are sensitive to liposomes of foreign DNA, the intrusion of which may lead to sudden death of the cells (Mortile, Passirani, Vonarbourg, Clavreul, & Benoit, 2008). From the results gotten so far, there is no clear indication that the transfection worked efficiently. Maybe other methods, such as electroporation and viral transfection, would have yielded more efficient results.

The viral method is the most widely used method, but it has its advantages and disadvantages. It has been reported that lentivirus vectors can efficiently infect both dividing and non-dividing cells. A lentivirus vector can infect the neural origin without damaging the function of the cells (Torashima, Okoyama, Nishizaki, & Hirai, 2006; Meunier & Pohl, 2009). The transgene (in this case the THP-1 cells) can have long term expression since the virus vector can be incorporated into the host cells (e.g THP-1 cells) genome stably (Cockrell & Kafri, 2007). The application of lentivirus is advantageous in accepting a large sequence of about 12 – 15 kb (Kumar, Keller, Makalou, & Sutton, 2001). Most importantly, unlike the liposomal transfection used in this thesis project study, lentivirus exhibits insignificant immunogenicity, in other words, it rarely instigates an immune reaction in the host cells. It is also compatible with many transcriptional promoters, including the promoters of the cells and the reference genes (Zheng et al., 2018). Despite the advantages of lentivirus vectors, there are also disadvantages. It is not easily accessible commercially, because of the safety risks. For example, the University of Skövde does not have the biosafety level of classification required for lentiviral experiments. Unlike liposomal transfection, lentivirus vectors are scarcely specific in binding to the region of interest, which could cause mutation and in turn lead to cancer development (Hargrove et al., 2008).

Taking inference from Figure 12, one can see that the NEK7 mRNA expression in sample TP (Transfected and primed) was -1.0 downregulated compared to the NEK7 mRNA expression in sample TU (Transfected and Un-primed). The Figure 12 shows that the ATP-activation of sample TPA indicates a 0.3 upregulation of NEK7 mRNA expression compared to the NEK7 mRNA expression in sample TP (Transfected and Primed). The stimulation of the samples with LPS and activation with ATP, was to enhance the NEK7 mRNA and the proteins expressions. However, one cannot determine the effect of the LPS-stimulation and the ATP-activation because the variations in the Ct values of the ACTB reference gene must have influenced the NEK7 mRNA expression results.

The NEK7 DNA knockout and the transfection were not concluded to have worked due to the inconsistency in the Ct values of the ACTB reference gene. Housekeeping genes such as ACTB are regarded to be reliable but many studies confirmed that these genes could vary in their expression in different situations (Lemay, Mao, & Singh,1996; Chang, Juan, Yin, Chi, & Tsay, 1998). This variation could be due to the fact that the housekeeping genes are involved in other functions, such as basal cell metabolism (Petersen, Rapaport, Henry, Huseman, & Moore, 1990). The ACTB reference gene discrepancy influenced the NEK7 mRNA expression results, which was the primary reason why the ELISA was not performed.

Conclusion

Interestingly, this thesis project did not conclude that CRISPR/Cas9 has worked substantially in NEK7 DNA knockout on human THP-1 cells. Rather it opens doors to repeat the experiment in the future to determine the efficiency of CRISPR/Cas9 in editing NEK7 DNA on human THP-1 Cells. This thesis project could not either establish that the transfection worked. Due to the variations of the ACTB reference gene, the research question in this thesis project "Could inflammasome function efficiently in absence of NEK7?" cannot be answered. However, several studies have considered the ACTB reference gene as the most stable on monocyte-like (THP-1) cells, but it depends on the experimental conditions of the study, such as environmental stress factors (e.g., heat) and tissues analysed. Therefore, it is advisable to determine the optimal experimental conditions before the commencement of every study.

Acknowledgements

I graciously thank God and my family who have fortified, encouraged and supported me immeasurably. This piece of knowledge would have not been possible without my supervisors, Mikael Ejdebäck and Matthew Herring, and my examiner, Maria Algerin.

References

Akond, Z., Alam, M., & Mollah, M. (2018). Biomarker Identification from RNA-Seq Data using a Robust Statistical Approach. *Bioinformation*, *14*(4), 153–163. https://doi.org/10.6026/97320630014153

Bauernfeind, F., Horvath, G., Stutz, A., Alnemri, E., MacDonald, K., Speert, D., & Fernandes-Alnemri, T. (2009). Cutting Edge: NF-κB Activating Pattern Recognition and Cytokine Receptors License NLRP3 Inflammasome Activation by Regulating NLRP3 Expression. *The Journal of Immunology*, *183*(2), 787-791.

Bustelo, M., Bruno, M., Loidl, C., Rey-Funes, M., Steinbusch, H., Gavilanes, A., & van den Hove, D. (2020). Statistical differences resulting from selection of stable reference genes after hypoxia and hypothermia in the neonatal rat brain. PLOS ONE, *15*(5), p.e0233387.

Cao, X., Luo, X., Liang, J., Zhang, C., Meng, X., & Guo, D. (2012). Critical selection of internal control genes for quantitative real-time RT-PCR studies in lipopolysaccharide-stimulated human THP-1 and K562 cells. *Biochemical and Biophysical Research Communications*, *427*(2), pp.366-372.

Cai, X., Chen, J., Xu, H., Liu, S., Jiang, Q., Halfmann, R., & Chen, Z. (2014). Prion-like Polymerization Underlies Signal Transduction in Antiviral Immune Defense and Inflammasome Activation. *Cell*, *156*(6), pp.1207-1222.

Chang, T., Juan, C., Yin, P., Chi, C., & Tsay, H. (1998). Up-regulation of beta-actin, cyclophilin and GAPDH in N1S1 rat hepatoma. *Oncology Reports*.

Chen, X., Liu, G., Yuan, Y., Wu, G., Wang, S., & Yuan, L. (2019). NEK7 interacts with NLRP3 to modulate the pyroptosis in inflammatory bowel disease via NF-κB signaling. *Cell Death & Disease*, *10*(12).

Chen, Y., Meng, J., Bi, F., Li, H., Chang, C., Ji, C., & Liu, W. (2019). Corrigendum: NEK7 Regulates NLRP3 Inflammasome Activation and Neuroinflammation Post-traumatic Brain Injury. *Frontiers in Molecular Neuroscience*, 12.

Cockrell, A., & Kafri, T. (2007). Gene delivery by lentivirus vectors. *Molecular Biotechnology*, *36*(3), 184-204.

Dinarello, C. (2009). Immunological and Inflammatory Functions of the Interleukin-1 Family. *Annual Review of Immunology*, *27*(1), 519-550. doi: 10.1146/annurev.immunol.021908.132612

Duncan, J., Bergstralh, D., Wang, Y., Willingham, S., Ye, Z., Zimmermann, A., & Ting, J. (2007). Cryopyrin/NALP3 binds ATP/dATP, is an ATPase, and requires ATP binding to mediate inflammatory signaling. *Proceedings Of The National Academy Of Sciences*, *104*(19), 8041-8046. doi: 10.1073/pnas.0611496104

Fernandes-Alnemri, T., Wu, J., Yu, J., Datta, P., Miller, B., Jankowski, W., ... Alnemri, S. E. (2007). The pyroptosome: a supramolecular assembly of ASC dimers mediating inflammatory cell death via caspase-1 activation. *Cell Death & Differentiation*, *14*(9), 1590-1604. doi: 10.1038/sj.cdd.4402194

Fink, S., & Cookson, B. (2006). Caspase-1-dependent pore formation during pyroptosis leads to osmotic lysis of infected host macrophages. *Cellular Microbiology*, *8*(11), 1812-1825. doi: 10.1111/j.1462-5822.2006. 00751.x

Franchi, L., Eigenbrod, T., Muñoz-Planillo, R., & Nuñez, G. (2009). The inflammasome: a caspase-1-activation platform that regulates immune responses and disease pathogenesis. *Nature Immunology*, *10*(3), 241-247. doi: 10.1038/ni.1703

Franchi, L., Eigenbrod, T., & Núñez, G. (2009). Cutting Edge: TNF-α Mediates Sensitization to ATP and Silica via the NLRP3 Inflammasome in the Absence of Microbial Stimulation. *The Journal of Immunology*, *183*(2), 792-796.

Franchi, L., Warner, N., Viani, K., & Nuñez, G. (2009). Function of Nod-like receptors in microbial recognition and host defense. *Immunological Reviews*, *227*(1), 106-128. doi: 10.1111/j.1600-065x.2008. 00734.x

González, M., Shaimar, R., Liu, C., Blankenship, H., & Zhu, G. (2020). Mouse Ptchd3 is a non-essential gene. *Gene: X*, 5, 100032.

Groskreutz, D., & Schenborn, E.T. (1997) Reporter systems. In: Tuan, R., *Methods in Molecular Biology 63*, 11ed., NJ, Humana Press.

Guo, H., Callaway, J., & Ting, J. (2015). Inflammasomes: mechanism of action, role in disease, and therapeutics. *Nature Medicine*, *21*(7), 677-687. doi: 10.1038/nm.3893

Haq, T., Richards, M., Burgess, S., Gallego, P., Yeoh, S., ... Bayliss, R. (2015). Mechanistic basis of Nek7 activation through Nek9 binding and induced dimerization. *Nature Communications*, *6*(1).

Hargrove, P., Kepes, S., Hanawa, H., Obenauer, J., Pei, D., Cheng, C., ... Persons, D. (2008). Globin Lentiviral Vector Insertions Can Perturb the Expression of Endogenous Genes in β-thalassemic Hematopoietic Cells. *Molecular Therapy*, *16*(3), 525-533.

He, W., Wan, H., Hu, L., Chen, P., Wang, X., Huang, Z., ... Han, J. (2015). Gasdermin D is an executor of pyroptosis and required for interleukin-1β secretion. *Cell Research*, *25*(12), 1285-1298. doi: 10.1038/cr.2015.139

He, Y., Zeng, M., Yang, D., Motro, B. and Núñez, G. (2016). NEK7 is an essential mediator of NLRP3 activation downstream of potassium efflux. *Nature*, *530*(7590), 354-357.

Henao-Mejia, J., Elinav, E., Jin, C., Hao, L., Mehal, W., Strowig, T., ... Flavell, A. R. (2012). Inflammasome-mediated dysbiosis regulates progression of NAFLD and obesity. *Nature*, *482*(7384), 179-185. doi: 10.1038/nature10809

Institute for Research in Immunology and Cancer. *Understanding qPCR results.* Retrieved 2020 May 10 from https://genomique.iric.ca/Infos_qPCR

Ishino, Y., Shinagawa, H., Makino, K., Amemura, M., & Nakata, A. (1987). Nucleotide sequence of the iap gene, responsible for alkaline phosphatase isozyme conversion in Escherichia coli, and identification of the gene product. *J Bacteriol*, 169, 5429–5433.

Juliana, C., Fernandes-Alnemri, T., Kang, S., Farias, A., Qin, F., & Alnemri, E. (2012). Non-transcriptional Priming and Deubiquitination Regulate NLRP3 Inflammasome Activation. *Journal of Biological Chemistry*, *287*(43), 36617-36622.

Kelley, N., Jeltema, D., Duan, Y., & He, Y. (2019). The NLRP3 Inflammasome: An Overview of Mechanisms of Activation and Regulation. *International Journal of Molecular Sciences*, *20*(13), 3328. doi: 10.3390/ijms20133328

Kim, S., Lee, K., & Rhee, K. (2007). NEK7 is a centrosomal kinase critical for microtubule nucleation. *Biochemical and Biophysical Research Communications*, *360*(1), 56-62.

Kumar, M., Keller, B., Makalou, N., & Sutton, R. E. (2001). Systematic determination of the packaging limit of lentiviral vectors. *Hum Gene Ther,* 12, 1893–1905.

Lamkanfi, M., & Dixit, V. (2014). Mechanisms and Functions of Inflammasomes. *Cell*, *157*(5), 1013-1022. doi: 10.1016/j.cell.2014.04.007

Lamkanfi, M., & Kanneganti, T. (2010). Nlrp3: An immune sensor of cellular stress and infection. *The International Journal of Biochemistry & Cell Biology*, *42*(6), 792-795. doi: 10.1016/j.biocel.2010.01.008

Lemay, S., Mao, C., & Singh, A. (1996). Cytokine gene expression in the MRL/lpr model of lupus nephritis. *Kidney International*, *50*(1), 85-93.

Liu, C., Zhang, L., Liu, H., & Cheng, K. (2017). Delivery strategies of the CRISPR-Cas9 gene-editing system for therapeutic applications. *Journal of Controlled Release*, *266*, 17-26. doi: 10.1016/j.jconrel.2017.09.012

Lopez-Castejon, G., Luheshi, N., Compan, V., High, S., Whitehead, R., Flitsch, S., … Brough, D. (2012). Deubiquitinases Regulate the Activity of Caspase-1 and Interleukin-1β Secretion via Assembly of the Inflammasome. *Journal of Biological Chemistry*, *288*(4), pp.2721-2733.

Martínez-Abraín, A. (2008). Statistical significance and biological relevance: A call for a more cautious interpretation of results in ecology. *Acta Oecologica, 34*(1), 9-11.

Medical News Today (2020). *Everything you need to know about inflammation.* Retrieved 2020 May 18 from https://www.medicalnewstoday.com/articles/248423#types-and-symptoms

Medzhitov, R. (2008). Origin and physiological roles of inflammation. *Nature*, *454*(7203), 428-435.

Menu, P., & Vince, J. (2011). The NLRP3 inflammasome in health and disease: the good, the bad and the ugly. *Clinical & Experimental Immunology*, *166*(1), 1-15. doi: 10.1111/j.1365-2249.2011.04440.x

Meunier, A., & Pohl, M. (2009). Lentiviral vectors for gene transfer into the spinal cord glial cells. *Gene Therapy,* 16, 476–482.

Miao, E., Leaf, I., Treuting, P., Mao, D., Dors, M., Sarkar, A., ... Aderem, A. (2010). Caspase-1-induced pyroptosis is an innate immune effector mechanism against intracellular bacteria. *Nature Immunology*, *11*(12), 1136-1142. doi: 10.1038/ni.1960

Morille, M., Passirani, C., Vonarbourg, A., Clavreul, A., & Benoit, J. (2008). Progress in developing cationic vectors for non-viral systemic gene therapy against cancer. *Biomaterials*, *29*(24-25), 3477-3496.

Olson, N., & Morrow, J. (2012). DNA extract characterization process for microbial detection methods development and validation. *BMC Research Notes*, *5*(1).

Park, E., Jung, H., Yang, H., Yoo, M., Kim, C., & Kim, K. (2007). Optimized THP-1 differentiation is required for the detection of responses to weak stimuli. *Inflammation Research*, *56*(1), 45-50.

Petersen, B., Rapaport, R., Henry, D., Huseman, C., & Moore, W. (1990). Effect of Treatment with Biosynthetic Human Growth Hormone (GH) on Peripheral Blood Lymphocyte Populations and Function in Growth Hormone-Deficient Children. *The Journal of Clinical Endocrinology & Metabolism*, *70*(6), 1756-1760.

Redman, M., King, A., Watson, C., & King, D. (2016). What is CRISPR/Cas9? Archives of Disease in Childhood - Education & Practice Edition, *101*(4), 213–215. doi:10.1136/archdischild-2016-310459

Sborgi, L., Ravotti, F., Dandey, V., Dick, M., Mazur, A., Reckel, S., … Hiller, S. (2015). Structure and assembly of the mouse ASC inflammasome by combined NMR spectroscopy and cryo-electron microscopy. *Proceedings of the National Academy of Sciences*, *112*(43), pp.13237-13242.

Schmid-Burgk, J., Chauhan, D., Schmidt, T., Ebert, T., Reinhardt, J., Endl, E., & Hornung, V. (2015). A Genome-wide CRISPR (Clustered Regularly Interspaced Short Palindromic Repeats) Screen Identifies NEK7 as an Essential Component of NLRP3 Inflammasome Activation. *Journal of Biological Chemistry*, *291*(1), 103-109.

Sessa, G., & Weissmann, G. (1968) Phospholipid spherules (liposomes) as a model for biological membranes. *J. Lipid Res.,* 9, 310–8.

Sharif, H., Wang, L., Wang, W., Magupalli, V., Andreeva, L., Qiao, Q., … Wu, H. (2019). Structural mechanism for NEK7-licensed activation of NLRP3 inflammasome. *Nature, 570*(7761), 338-343.

Sharma, D., & Kanneganti, T. (2016). The cell biology of inflammasomes: Mechanisms of inflammasome activation and regulation. *The Journal of Cell Biology*, *213*(6), 617-629. doi: 10.1083/jcb.201602089

Shi, H., Wang, Y., Li, X., Zhan, X., Tang, M., Fina, M., … Beutler, B. (2015). NLRP3 activation and mitosis are mutually exclusive events coordinated by NEK7, a new inflammasome component. *Nature Immunology*, *17*(3), 250-258.

Thomas, P., Dash, P., Aldridge, J., Ellebedy, A., Reynolds, C., Funk, A., ... Kanneganti, T. (2009). The Intracellular Sensor NLRP3 Mediates Key Innate and Healing Responses to Influenza A Virus via the Regulation of Caspase-1. *Immunity*, *30*(4), 566-575. doi: 10.1016/j.immuni.2009.02.006

Tilevik, A. (n.d.). Calculations Based on qPCR Data. Institutionen för Biovetenskap, Högskolan i Skövde. Retreived 2020 June 7 from http://websvrnu.his.se/jana/qPCR/qPCR.html

Torashima, T., Okoyama, S., Nishizaki, T., & Hirai, H. (2006). In vivo transduction of murine cerebellar Purkinje cells by HIV-derived lentiviral vectors. *Brain Res,* 1082, 11–22.

Vajjhala, P., Mirams, R., & Hill, J. (2012). Multiple Binding Sites on the Pyrin Domain of ASC Protein Allow Self-association and Interaction with NLRP3 Protein. *Journal of Biological Chemistry*, *287*(50), 41732-41743. doi: 10.1074/jbc.m112.381228

Vaure, C., & Liu, Y. (2014). A comparative review of toll-like receptor 4 expression and functionality in different animal species. *Frontiers in immunology*, *5*, 316. doi:10.3389/fimmu.2014.00316

Wilfinger, W., Mackey, K., & Chomczynski, P. (1997). Effect of pH and Ionic Strength on the Spectrophotometric Assessment of Nucleic Acid Purity. *BioTechniques*, *22*(3), 474-481.

World Medical Association (WMA) of Helsinki Declaration (2018). Ethical Principles for Medical Research Involving Human Subjects. Retrieved 2020 August 2 from https://www.wma.net/policies-post/wma-declaration-of-helsinki-ethical-principles-for-medical-research-involving-human-subjects/

Yissachar, N., Salem, H., Tennenbaum, T., & Motro, B. (2006). Nek7 kinase is enriched at the centrosome, and is required for proper spindle assembly and mitotic progression. *FEBS Letters*, *580*(27), 6489-6495.

Zhou, L., Wang, Z., Xu, X., Wan, Y., Qu, K., Fan, H., ... Liu, C. (2016). Nek7 is overexpressed in hepatocellular carcinoma and promotes hepatocellular carcinoma cell proliferation in vitro and in vivo. *Oncotarget*, *7*(14). doi: 10.18632/oncotarget.7620

Zheng, C., Wang, S., Bai, Y., Luo, T., Wang, J., Dai, C., … Wang, Y. (2018). Lentiviral Vectors and Adeno-Associated Virus Vectors: Useful Tools for Gene Transfer in Pain Research. *The Anatomical Record*, *301*(5), 825-836.

Appendix

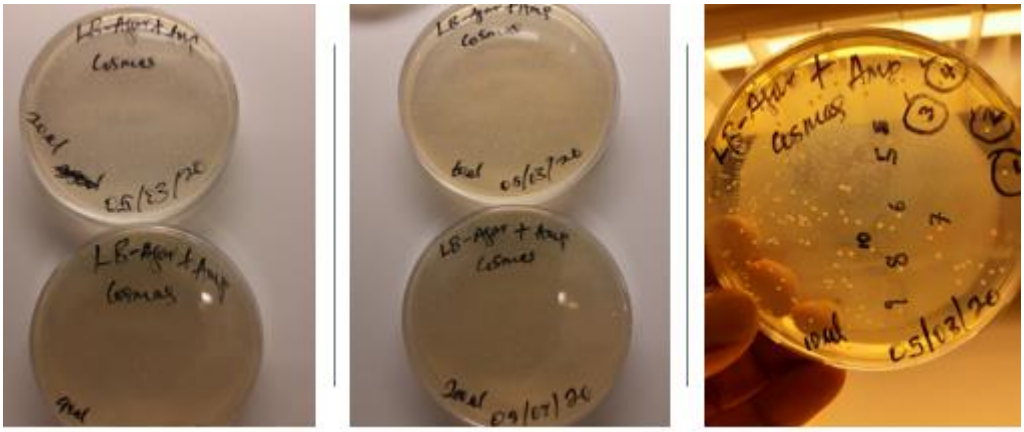

Figure 1. Growth of colonies in LB-agar ampicillin plates of varieties of volumes of recombinant DNA

Sample c			Avg ct	SD	
NU		25.37	25.39	0.094516	
NU		25.41			
NU		25.23			Δct
					7.115
			Avg ct	SD	
NU ACTB		17.14	17.89667	0.656836	
NU ACTB		18.23	18.275	0.06364	
NU ACTB		18.32			

			Avg ct	SD	
NP		26.58	26.565	0.021213	
NP		26.55			
NP		27.18	26.77	0.290172	Δct
					8.111667
			Avg ct	SD	
NP ACTB		18.32	18.45333	0.117189	
NP ACTB		18.5			
NP ACTB		18.54			

			Avg ct	SD	
NPA		24.46	24.33333	0.120554	
NPA		24.22			
NPA		24.32			Δct
					8.18
			Avg ct	SD	
NPA ACTB		16.08	16.15333	0.135769	
NPA ACTB		16.07			
NPA ACTB		16.31			

			Avg ct	SD	
TU		25.31	25.22	0.081854	
TU		25.15			
TU		25.2			Δct
					7.556667
			Avg ct	SD	
TU ACTB		17.49	17.66333	0.226789	
TU ACTB		17.58			
TU ACTB		17.92			

			Avg ct	SD	
TP		27.5	25.925	0.90934	
TP		25.92	25.925	0.007071	
TP		25.98			Δct
					8.518333
			Avg ct	SD	
TP ACTB		17.33	17.40667	0.100167	
TP ACTB		17.37			
TP ACTB		17.52			

			Avg ct	SD	
TPA		27.49	27.34	0.106066	
TPA		27.34			
TPA		NaN			Δct
					7.26
			Avg ct	SD	
TPA ACTB		NaN	20.08	0.098995	
TPA ACTB		20.01			
TPA ACTB		20.15			

			Avg ct	SD	
CU		26.86	26.495	0.245017	
CU		26.37			
CU		26.62			Δct
					7.555
			Avg ct	SD	
CU ACTB		18.95	18.94	0.036056	
CU ACTB		18.9			
CU ACTB		18.97			

			Avg ct	SD	
CP		27.57	27.25	0.231517	
CP		27.15			
CP		27.03			Δct
					7.013333
			Avg ct	SD	
CP ACTB		20.23	20.23667	0.180093	
CP ACTB		20.06			
CP ACTB		20.42			

			Avg ct	SD	
CPA		28.46	27.88333	0.407949	
CPA		27.61	27.595	0.021213	
CPA		27.58			Δct
					6.235
			Avg ct	SD	
CPA ACTB		22.07	21.59667	0.419682	
CPA ACTB		21.27	21.36	0.127279	
CPA ACTB		21.45			

Figure 2. Raw qPCR data